

CHEMISTRY

A European Journal

A Journal of



Accepted Article

Title: Light-induced spin transitions in copper-nitroxide-based switchable molecular magnets: insights from periodic DFT+U calculations

Authors: Rocío Sánchez-de-Armas, Norge Cruz-Hernández, and Carmen J. Calzado

This manuscript has been accepted after peer review and appears as an Accepted Article online prior to editing, proofing, and formal publication of the final Version of Record (VoR). This work is currently citable by using the Digital Object Identifier (DOI) given below. The VoR will be published online in Early View as soon as possible and may be different to this Accepted Article as a result of editing. Readers should obtain the VoR from the journal website shown below when it is published to ensure accuracy of information. The authors are responsible for the content of this Accepted Article.

To be cited as: *Chem. Eur. J.* 10.1002/chem.201803962

Link to VoR: <http://dx.doi.org/10.1002/chem.201803962>

Supported by
ACES

WILEY-VCH

Light-induced spin transitions in copper-nitroxide-based switchable molecular magnets: insights from periodic DFT+U calculations

Rocío Sánchez-de-Armas,^a Norge Cruz Hernández,^b Carmen J. Calzado^{a*}

^aDepartamento de Química Física. Universidad de Sevilla. 41012. Spain.

^bDepartamento de Física Aplicada I, Escuela Politécnica Superior, Universidad de Sevilla, 41011, Spain

*corresponding author: calzado@us.es

Abstract

The electronic structure and magnetic interactions of three representative members of the breathing crystal $\text{Cu}(\text{hfac})_2\text{L}^{\text{R}}$ family, mainly $\text{Cu}(\text{hfac})_2\text{L}^{\text{Pr}}$ (**1**), $\text{Cu}(\text{hfac})_2\text{L}^{\text{Bu}}\cdot 0.5\text{C}_8\text{H}_{18}$ (**2**) and $\text{Cu}(\text{hfac})_2\text{L}^{\text{Bu}}\cdot 0.5\text{C}_8\text{H}_{10}$ (**3**), have been analyzed by means of periodic plane-wave based DFT+U calculations. These copper(II)-nitroxide based molecular magnets display promising thermally and optically induced switchable behaviour, similar to the spin-crossover and light-induced excited spin state trapping phenomena. The calculations confirm the presence of temperature-dependent exchange interaction within the spin triads formed by the three-spin nitronyl nitroxide-copper(II)-nitronyl nitroxide units, in line with the changes observed in the effective magnetic moment when temperature increases. Moreover, they quantify the interchain interaction mediated by the terminal nitroxide group of two spin triads in neighbour polymer chains. This interaction competes with the exchange interaction within the spin triads at high temperature and introduces 1D exchange channels that do not coincide with the polymeric chains. The density of states reveal that the low-lying conduction states potentially involved in the UV-vis transitions are mainly located on the nitronyl-nitroxide radicals, the hfac groups and the Cu atoms. Then, the density of states is almost independent of the solvent and the R group substituting the pyrazole moiety, which suggests the possibility of light-induced spin switching for other members of the breathing crystal family. The band at 500 nm characterizing the strongly-coupled low-temperature phase can be ascribed to a ligand-to-metal charge transfer transition between the nitronyl-nitroxide and the Cu bands. This study appears to be fundamental in order to properly understand the optical properties of these switching molecular magnets.

Accepted Manuscript

1. Introduction

Switchable molecular compounds attracted much attention in last several decades due to their potential applications in magnetic data storage, quantum computing, spintronics and related areas.^[1] Spin-crossover (SCO) complexes are among the most promising candidates, most of them based on iron(II), where the switching between different spin states can be induced by different external stimuli such as temperature, pressure or light.^{[2],[3]} In fact, to date the light-induced excited spin state trapping (LIESST) phenomenon has mostly been observed on SCO complexes of iron(II)^{[4],[5]} and iron(III).^{[6],[1]}

Recently, a family of switchable compounds with SCO-like behaviour and LIESST-like phenomena based on Cu(II) and nitronyl nitroxide (NIT) ligands have been reported.^{[7],[8],[9],[10],[11],[12],[13],[14]} These compounds of formula $\text{Cu}(\text{hfac})_2\text{L}^{\text{R}}$ consist of heterospin polymer-chain complexes of Cu(II) hexafluoroacetylacetonato (hfac) with stable pyrazole-substituted nitronyl nitroxides, L^{R} , with R=Me, Et, Pr, i-Pr, Bu. Two different motifs of the polymer chains can be obtained (Figure 1): a head-to-tail motif leading to the formation of two-spin Cu(II)-nitroxide clusters, and a head-to-head motif, resulting in alternating one-spin Cu(II) and three-spin NIT-Cu(II)-NIT clusters (spin triads).

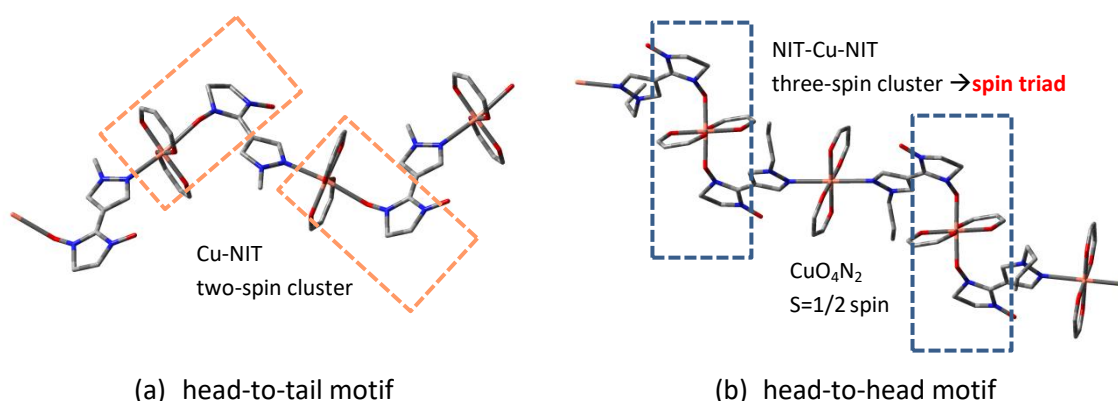


Figure 1. Head-to-tail (a) and head-to-head (b) motifs in the heterospin $\text{Cu}(\text{hfac})_2\text{L}^{\text{R}}$ polymer-chain complexes. Red, blue, gray and orange tubes represent O, N, C and Cu atoms, respectively. Orange and blue boxes represent the two-spin Cu-NIT clusters and three-spin NIT-Cu-NIT clusters, respectively. Hydrogen atoms, $-\text{CF}_3$ and $-\text{CH}_3$ groups have been omitted for clarity.

These $\text{Cu}(\text{hfac})_2\text{L}^{\text{R}}$ systems present magnetic anomalies that can be thermally and optically induced, similar to the classical spin-crossover, but different in nature. The crystal undergoes reversible structural rearrangements, that modify the exchange interaction between the Cu(II) and the nitroxide spins when the temperature changes (Figure 2). At high temperatures the spins are weakly ferromagnetically coupled (weakly exchange-coupled state, WS), with $J \approx 10\text{--}20\text{ cm}^{-1}$,^{[15],[16]} whereas at low temperatures the Cu(II) and the nitroxide spins are coupled by a strong antiferromagnetic interaction,^[16] with $J \approx -100\text{--}200\text{ cm}^{-1}$, and the spin triad converts to the strongly coupled spin state with a total spin $S=1/2$ (strongly exchange-coupled state, SS). As a result, the effective magnetic moment μ_{eff} decreases when the temperature drops (Figure 2). The change of the magnetic moment $\Delta\mu_{\text{eff}}$ can be gradual or abrupt depending on R^[17] and the solvent. The impact of the solvent has been associated to the relative orientation of the

solvent molecules with respect to the spin triads.^{[18],[19]} The large difference in Cu-O bond lengths between SS and WS states is responsible for the significant change of the unit cell volume during the spin transition, and for this reason these systems have been called *breathing crystals*.^[10]

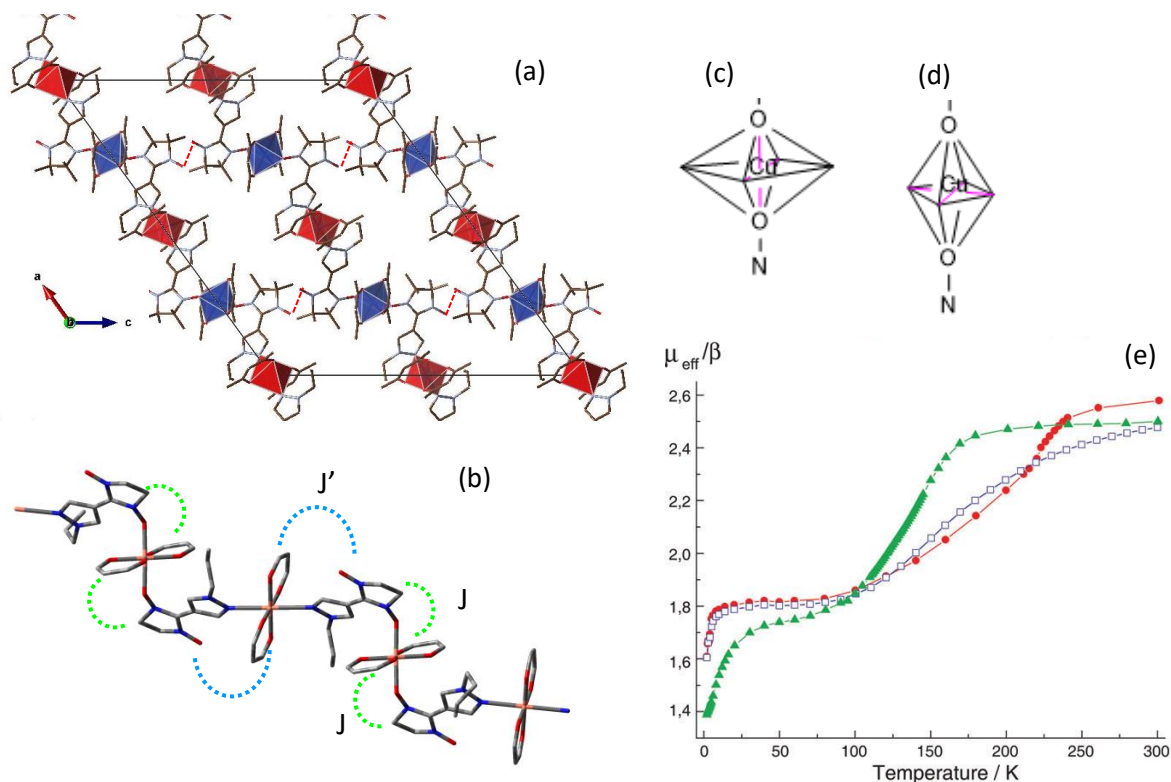


Figure 2. (a) View along b axis of the $\text{Cu}(\text{hfac})_2\text{L}^{\text{Pr}}$ complex. H and F atoms are omitted for clarity. Blue and red polyhedra represent CuO_6 and CuO_4N_2 octahedron, respectively. The dotted red lines represent the interchain interactions. (b) Magnetic interactions along the polymer chain. The dotted green and blue lines represent the Cu-NIT interaction within the triad (J) and the interaction between the spin-triad and the one-spin CuO_4N_2 cluster (J'). Schematic representation of the elongated octahedral CuO_6 sites in the spin triad for the LT (c) and HT (d) phases. (e) Temperature dependence of the effective magnetic moment $\mu_{\text{eff}}(T)$ of $\text{Cu}(\text{hfac})_2\text{L}^{\text{Pr}}$ (**1**) (red circles), $\text{Cu}(\text{hfac})_2\text{L}^{\text{Bu}} \cdot 0.5\text{C}_8\text{H}_{10}$ (**2**) (blue squares), $\text{Cu}(\text{hfac})_2\text{L}^{\text{Bu}} \cdot 0.5\text{C}_8\text{H}_{18}$ (**3**) (green triangles). Reproduced from Ref. ^[20] with permission from the PCCO Owner Societies.

The photoswitching in the $\text{Cu}(\text{hfac})_2\text{L}^{\text{R}}$ family has been observed for the first time for $\text{Cu}(\text{hfac})_2\text{L}^{\text{Pr}}$ complex,^[12] and also documented for $\text{Cu}(\text{hfac})_2\text{L}^{\text{Bu}}$ with propyl-benzene and *m*-xylene as solvents^[21] using EPR^{[12],[21]} and time-resolved EPR.^[22] The phenomenon has also been reported on a related polymer chain complex of $\text{Cu}(\text{hfac})_2$ with tert-butylpyrazolyl nitroxide radical.^[23] Illumination with light at very low temperature induced a metastable WS state, where the system remains trapped for hours. The relaxation to the ground SS state is nonexponential and has a self-decelerating character.^[21] The process has been also analysed by femtosecond optical spectroscopy for $\text{Cu}(\text{hfac})_2\text{L}^{\text{Pr}}$ complex.^[13] Figure 3 shows the UV-vis absorption spectra of the WS and SS states of $\text{Cu}(\text{hfac})_2\text{L}^{\text{Pr}}$ which are dominated by the nitronyl nitroxide bands in the $\lambda=450\text{-}700$ nm region.^{[14],[13]} Similar UV-vis spectra have been reported for the related $\text{Cu}(\text{hfac})_2\text{L}^{\text{Me}}$ and $\text{Cu}(\text{hfac})_2\text{L}^{\text{Et-CP}}$ complexes.^[14] The most significant difference between both states is a strong band at $\lambda=500$ nm observed only at low temperature (SS

state), and tentatively assigned to a charge transfer band (metal-to-ligand^[13] or ligand-to-metal^{[13],[14]}). A further feature is the displacement of the structure band centered at ~650 nm, associated with the nitroxide radicals, to a higher energy.^[14] The bleaching of optical density in the $\lambda=500-600$ nm region has been employed to monitor the photoinduced SS \leftrightarrow WS conversion and provide information about its timescale. A three-state mechanism involving the SS, WS and the photoexcited E* states has been suggested, but the nature of this E* state has not been identified, and then the mechanism of the ultrafast spin state photoswitching is far from being fully understood to date.^{[22],[23],[13]}

In this context, information regarding the available electronic states that could connect the SS and WS states in the photoinduced transition would be extremely useful. At present, theoretical studies of breathing crystals are scarce, and have been mostly oriented to the evaluation of the coupling within the spin triads and the interchain couplings using different approaches such as the difference dedicated configuration interaction (DDCI) method,^[24] CASPT2,^[25] or broken symmetry DFT-based calculations.^{[19],[26]} Regarding periodic treatments, it is worth mentioning a recent study by Morozov *et al.*^[27] where the periodic GGA+U approach has been applied to describe the magnetic coupling within the spin triads of two related Cu(hfac)₂L^{Me} and Cu(hfac)₂L^{Et} polymer chains. A reduced crystal symmetry was employed to decrease the number of atoms in the unit cell and consequently the computational cost, but in doing so the interchain interactions are neglected.

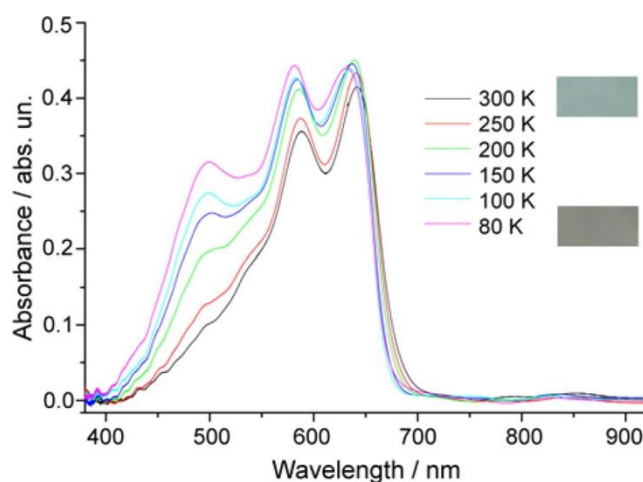


Figure 3. UV-Vis absorption spectra of Cu(hfac)₂L^{Pr} (**1**) recorded at 80-300K. Reprinted with permission from Ref. ^[22]. Copyright 2012 American Chemical Society.

Therefore, the aim of this work is to obtain a reliable description of the electronic structure of the breathing crystal from *state-of-the-art* quantum chemistry approaches. We use plane wave-based periodic calculations for three representative members of the breathing crystal Cu(hfac)₂L^R family: Cu(hfac)₂L^{Pr} (**1**), Cu(hfac)₂L^{Bu}·0.5C₈H₁₈ (**2**) and Cu(hfac)₂L^{Bu}·0.5C₈H₁₀ (**3**). Our DFT+U calculations on the low and high temperature phases provide information about the relative stability of different spin arrangements in the spin triads and the isolated CuO₄N₂ units, estimates of the magnetic coupling interactions between the nitroxide and Cu(II) spins

within the triads and confirm the presence of antiferromagnetic interactions between the polymeric chains mediated by the terminal nitronyl-nitroxide groups. Additionally, the density of states furnishes key features of the low-lying electronic states of the low-temperature (LT) and high-temperature (HT) phases that could help in the elucidation of the states involved in the photoswitching process and could get insight into its whole mechanism. The density of states reveal that the low-lying conduction states potentially involved in the UV-vis transitions are mainly located on the nitronyl-nitroxide radicals, the hfac groups and the Cu atoms. i.e. located on common components of all the members of the breathing crystal family. Then, the density of states is almost independent of the solvent and the R group substituting the pyrazole moiety. Hence, the similarities found in the density of states for these three compounds suggest the potential occurrence of the LIESST-like phenomenon in other members of the breathing crystal family.

2. Description of the systems

Three compounds $\text{Cu}(\text{hfac})_2\text{L}^{\text{Pr}}$, $\text{Cu}(\text{hfac})_2\text{L}^{\text{Bu}}\cdot 0.5\text{C}_8\text{H}_{18}$ and $\text{Cu}(\text{hfac})_2\text{L}^{\text{Bu}}\cdot 0.5\text{C}_8\text{H}_{10}$ (**1-3**) of the breathing crystal family have been considered, which have been extensively characterized in the past by X-ray diffraction, SQUID magnetometry, EPR and UV-Vis spectroscopies.^{[28],[29],[19],[11],[12],[30],[31],[20],[15],[21],[13]} In all cases, the polymer chains present a head-to-head coordination motif with alternating one-spin Cu(II) in CuO_4N_2 units and three-spin nitroxide-Cu(II)-nitroxide CuO_6 clusters (Figure 2a). Compounds **1-3** differ on the R substituent of the nitroxide ligand (R=Pr for **1**, Bu for **2** and **3**) and the organic solvent (*solv*) included into the crystal structure (*solv*=octane C_8H_{18} for **2** and *ortho*-xylene C_8H_{10} for **3**), and have been selected as representative examples of the differential role of both the substituent^[17] and the solvent^{[18],[19]} on the magnetostructural transition.

At low temperature the nitronyl-nitroxide radicals occupy equatorial positions in the elongated CuO_6 octahedral units (Figure 2c), while they occupy the axial position in the CuO_6 octahedron in the high temperature structure (Figure 2d). As a result of the rotation of the elongated Jahn-Teller axis in the CuO_6 octahedron with temperature, the Cu-nitroxide distances are elongated and more importantly the Cu 3d and π -nitroxide orbitals carrying the unpaired electrons adopt a quasi-orthogonal relative orientation, as demonstrated the *ab initio* calculations carried out by one of us in the $\text{Cu}(\text{hfac})_2\text{L}^{\text{Bu}}\cdot 0.5\text{C}_8\text{H}_{18}$ (**2**) complex.^[24] Table 1 shows the Cu-O bond distances in the CuO_6 octahedron for the two structures considered (LT and HT phases) for each compound. Also the bond angle between the nitroxide group and the Cu ion is reported for each structure. Additional structural information is reported in Table S1 for compounds **1-3**, together with plots of the unit cell for both phases in Figure S1. Consequently, these structural changes have a dramatic impact on the exchange interactions between the Cu and nitronyl-nitroxide spins in the triad, which are significantly modified during the $\text{SS} \leftrightarrow \text{WS}$ conversion. By contrast, the one-spin CuO_4N_2 units remain magnetically isolated in all range of temperatures.

The three compounds experience gradual magnetostructural transitions, i.e. the magnetic susceptibility changes smoothly with temperature (Figure 2e). The complex $\text{Cu}(\text{hfac})_2\text{L}^{\text{Pr}}$ (**1**) presents a gradual transition on a broad temperature range $T=100\text{-}250\text{K}$.^[10] Moreover, a structural phase transition occurs at $T=226\text{K}$,^{[28],[11]} the crystal belongs to the $\text{P2}_1/\text{c}$ space group at low temperature while the space symmetry group is $\text{C2}/\text{c}$ at $T > 226\text{K}$. The complex

$\text{Cu}(\text{hfac})_2\text{L}^{\text{Bu}}\cdot\text{C}_8\text{H}_{10}$ (**3**) has a similar behaviour, although the transition region is broader (100-300K), and the transition temperature is shifted by $\sim 60\text{K}$ to lower temperatures. Complex $\text{Cu}(\text{hfac})_2\text{L}^{\text{Bu}}\cdot\text{C}_8\text{H}_{18}$ (**2**) represents an intermediate case between abrupt and gradual spin transition,^[11] with a narrower temperature range, 75-175K, and a transition temperature of $\sim 130\text{K}$.^[19]

Table 1. Main geometrical parameters within the spin triad for the LT and HT structures of compounds **1-3**. Cu-O_L and $\text{Cu-O}_{\text{hfac}}$ represent the bond distances between the Cu and O atoms in the nitronyl-nitroxide and hfac groups, respectively. All parameters from X-ray diffraction data.^{[11],[20]}

$\text{Cu}(\text{hfac})_2\text{L}^{\text{R}}\cdot\text{so}/\text{v}$	T (K)	Cu-O_L (Å)	$\text{Cu-O}_L\text{-N}(\text{°})$	$\text{Cu-O}_{\text{hfac}}$ (Å)	$\text{Cu-O}_{\text{hfac}}$ (Å)
1 R=Pr	50	1.994	123.3	2.274	1.949
	240	2.256	127.1	2.018	1.960
2 R=Bu, so/v=octane	100	2.034	123.1	2.201	1.998
	295	2.352	125.3	1.971	1.961
3 R=Bu, so/v=o-xylene	60	2.003	126.1	2.301	1.963
	240	2.206	128.5	2.004	1.975

3. Computational details

The crystals have been studied within density functional theory (DFT) using the Vienna *ab initio* simulation package (VASP) code,^{[32],[33],[34],[35]} employing the generalized gradient approximation (GGA) with the Perdew-Burke-Ernzerhof exchange-correlation functional^[36] and projector-augmented wave (PAW) potentials.^{[37],[38]} Effective Hubbard corrections of 9.8 eV and 5 eV have been used to describe the localized Cu 3d orbitals and O 2p orbitals respectively, using Dudarev's approach,^[39] as in the previous study by Morozov *et al.*^{[27],[40]} on the related $\text{Cu}(\text{hfac})_2\text{L}^{\text{Me}}$ and $\text{Cu}(\text{hfac})_2\text{L}^{\text{Et}}$ compounds. The PBE+U method is considered as a practical alternative to hybrid methods when plane-wave basis sets are used, where the evaluation of the Fock exchange terms is computationally prohibitive.^{[41],[42],[43]} The main weakness of the +U correction is precisely the choice of U. Some attempts have been made in the past for obtaining estimates of the U value from an unbiased and independent evaluation based on extended CI calculations on representative fragments of the system.^[44] However, this approach does not work for the breathing crystals, due to the π nature of the active orbitals of the nitronyl-nitroxide radicals, responsible for a frame of low-lying states in competition with those required for the evaluation of U. Instead, we have checked the impact of the U value by a complementary set of calculations with $U(\text{Cu})=2, 7$ and 9.8 eV.

Valence electrons are described using a plane-wave basis set with a cutoff of 500 eV and a Γ -centred grid of k-points is used for integrations in the reciprocal space, where the smallest allowed spacing between k-points is set at 0.2 \AA^{-1} .^[45] Van der Waals interactions were taken into account through the Tkatchenko-Scheffler method.^[46] Hereafter, PBE+ $U_d(n)$ refers to calculations with $U=n$ eV correction in Cu 3d orbitals and PBE+ U_d+U_p refers to calculations with $U_d=9.8$ eV for Cu 3d and $U_p=5$ eV for O 2p orbitals, including Van der Waals corrections in all cases.

For each crystal we have considered the experimental structure^{[11],[20]} at two temperatures representative of the LT and HT structures (50 K and 240 K, 100 K and 295 K, 60 K and 240 K for compounds **1-3**, respectively) and single-point calculations have been done for different magnetic solutions. Electronic relaxation has been performed until the change in the total energy between two consecutive steps is smaller than 10^{-6} eV. Unlike the previously reported periodic calculations on breathing crystals,^{[11],[29],[20]} in our calculations the experimental space group for each system is employed ($P\bar{1}$ for compounds **2** and **3** in both temperatures,^{[11],[20]} $P2_1/c$ and $C2/c$ for compound **1** at low and room temperatures,^[29] respectively), with unit cells of 552, 170 and 162 atoms for compounds **1**, **2** and **3** respectively. Hence, our calculations take into account the interchain interactions, neglected in the works by Morozov *et al.*^[27] as a consequence of the reduced crystal symmetry used in their calculations.

4. Results

Periodic plane wave-based PBE+U calculations have been performed to establish the electronic structure at low and high temperatures of three members of the $\text{Cu}(\text{hfac})_2\text{L}^{\text{R}}$ family. The goal is two-fold: first, to establish a reliable procedure for describing the whole crystal, explicitly including the interchain interactions, relevant in the description of the spin dynamics and second, to interpret the origin of the main bands on the UV-Vis spectra with a potential role in the photoswitching process.

4.1. Impact of the U value on the relative energies of the magnetic solutions

Comparing with calculations on fragments modeling the spin triads,^{[24],[25],[19],[26]} the periodic calculations are free of border effects, take into account all the groups and atoms of the real crystal without any simplification, and explicitly deal with the interchain interactions, considered as relevant for the spin dynamics at high temperature. However DFT based periodic calculations are functional-dependent and in the case of DFT+U calculations, the choice of U is a relevant step. Four different U values are considered, as described above, and their impact on the (i) relative energy of the magnetic solutions for the LT and HT structures, (ii) density of states, and (iii) amplitude and nature of the magnetic interactions will be analyzed.

Table 2. Relative stability (per NIT-Cu-NIT...Cu units) and magnetic coupling constants for $\text{Cu}(\text{hfac})_2\text{L}^{\text{R}}\cdot\text{sol}/v$ compounds (**1-3**) at PBE+ U_d+U_p level. Intracluster coupling J , the interaction between the spin triad and the CuO_4N_2 units J' and the interchain interactions J_{chain} are reported. All values are in cm^{-1} .

$\text{Cu}(\text{hfac})_2\text{L}^{\text{R}}\cdot\text{sol}/v$	Phase	AFM	AFM2	FM	J	J'	J_{chain}
1 R=Pr	LT	0.0	0.0	737.0	-368.9	0.0	-2.8
	HT	27.8	27.8	0.0	13.5	0.0	
2 R=Bu, $\text{sol}/v=\text{octane}$	LT	0.0	-10.1	520.5	-260.2	-10.1	
	HT	38.5	38.5	0.0	19.3	0.0	
3 R=Bu, $\text{sol}/v=\text{o-xylene}$	LT	0.0	0.1	644.4	-322.2	0.1	
	HT	48.2	48.2	0.0	24.1	0.0	-5.8

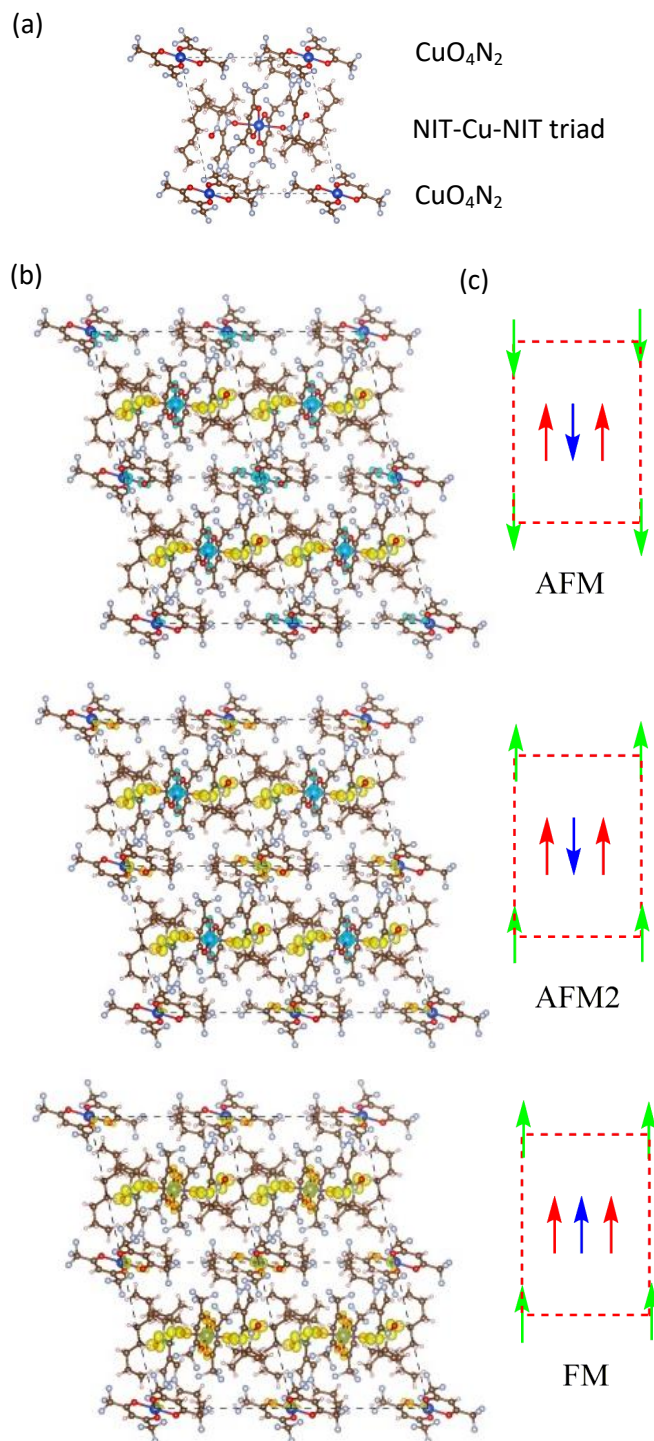


Figure 4. (a) View along the a axis of the unit cell for compound **2**, in the middle the nitroxide-Cu-nitroxide spin triad, and in the corners the one-spin CuO_4N_2 clusters. (b) Spin density maps of compound **2** for the AFM (top), AFM2 (middle) and FM (bottom) solutions. Four unit cells are represented, delimited by a dashed line. View along the a axis. (c) Schematic representation of the three considered magnetic solutions for compounds **2** and **3**. Blue and red arrows represent, respectively, the Cu and nitronyl-nitroxide spins of the three-spin cluster (spin triad). Green arrow represents the one-spin CuO_4N_2 cluster.

The unit cell for $\text{Cu}(\text{hfac})_2\text{L}^{\text{Bu}}\cdot 0.5\text{C}_8\text{H}_{18}$ (**2**) and $\text{Cu}(\text{hfac})_2\text{L}^{\text{Bu}}\cdot 0.5\text{C}_8\text{H}_{10}$ (**3**) compounds contains four unpaired electrons, three on the spin triad and one on the CuO_4N_2 unit. Hereafter Cu1 and Cu2 represent the copper atom in the spin triad and CuO_4N_2 units, respectively. Three different magnetic solutions have been calculated, corresponding to different spin distributions $|\text{NIT-Cu1-NIT}\dots\text{Cu2}|$ (Figure 4 for compound **2**, Figure S2 for compound **3**). Table 2 reports the results obtained for $\text{PBE}+U_d+U_p$. The rest of explored U values can be found in Tables S2 and S3. At low temperature, the ground state corresponds to the AFM solution with $S_z=0$, $|\uparrow\uparrow\uparrow\dots\downarrow|$, where the two nitronyl-nitroxide groups present an antiferromagnetic coupling with the Cu1 centre, and the two Cu centers are coupled ferromagnetically. This solution is almost degenerate with the AFM2 solution $|\uparrow\downarrow\uparrow\dots\uparrow|$ with $S_z=1$, differing from the AFM solution by the relative orientation of the Cu spins. This confirms that the CuO_4N_2 clusters are magnetically isolated. The ferromagnetic solution $|\uparrow\uparrow\uparrow\dots\uparrow|$ with $S_z=2$ is high in energy, as expected for the low-temperature strongly-coupled phase. At high temperature, the three solutions are almost degenerate the ferromagnetic solution being the most stable one (Table 2). Again this result is in agreement with the experimental data for the high-temperature weakly-coupled phase. Additionally, in the case of $\text{Cu}(\text{hfac})_2\text{L}^{\text{Bu}}\cdot 0.5\text{C}_8\text{H}_{10}$, it has been possible to isolate an additional solution (AFM4) for the HT structure, corresponding to the distribution $|\uparrow\uparrow\downarrow\dots\uparrow|$ (Figure S2). When this distribution is replicated, the interaction between the terminal NO groups of two neighbor spin triads is antiferromagnetic, while in the rest of considered broken-symmetry solutions, all the interactions between neighbor spin triads are ferromagnetic (Figure S2). This solution provides additional information about the amplitude and nature of the interchain interaction mediated by the terminal nitroxide groups in two neighbour chains.

In the case of the $\text{Cu}(\text{hfac})_2\text{L}^{\text{Pr}}$ (**1**) complex, the unit cell contains four spin triads and four CuO_4N_2 units. The four considered solutions are schematically represented in Figure 5, together with the projections of the spin density on the *ac* plane. Solution AFM3 differs from AFM2 by the antiferromagnetic interchain interaction, J_{chain} . The relative energy of the four solutions with different U values is shown in Table 3. They present a strong dependence on the U value for the LT structures, while the energy gaps are almost insensitive to U for the HT solutions except for $\text{PBE}+U_d(2)$. The relative energy of the explored solutions are in good agreement with the experimental data, except for $\text{PBE}+U_d(2)$ where an AFM ground state is predicted at HT, although the AFM-FM gap is strongly modulated by the chosen U value. At low temperature, AFM3 solution is the most stable one, which indicates the presence of an antiferromagnetic interchain interaction as obtained for $\text{Cu}(\text{hfac})_2\text{L}^{\text{Bu}}\cdot 0.5\text{C}_8\text{H}_{10}$ (**3**). This AF interchain interaction has been also evidenced in our previous theoretical study on $\text{Cu}(\text{hfac})_2\text{L}^{\text{Bu}}\cdot 0.5\text{C}_8\text{H}_{18}$ (**2**).^[24] Hence, in these systems the chains are magnetically connected through the terminal nitroxide groups of the three-spin clusters of two neighbouring chains. This intercluster interaction gives 1D exchange channels that do not coincide with the polymeric chains but rather spread across them.^[26] The presence of this interaction is of vital importance for the interpretation of the spin dynamics and relaxation of the photoinduced WS state at low temperature, as discussed below. Since the NO...NO contacts among the polymer-chains are ubiquitous to all these compounds, it is reasonable to suggest that this 1D magnetic ordering is a common feature of the whole family.

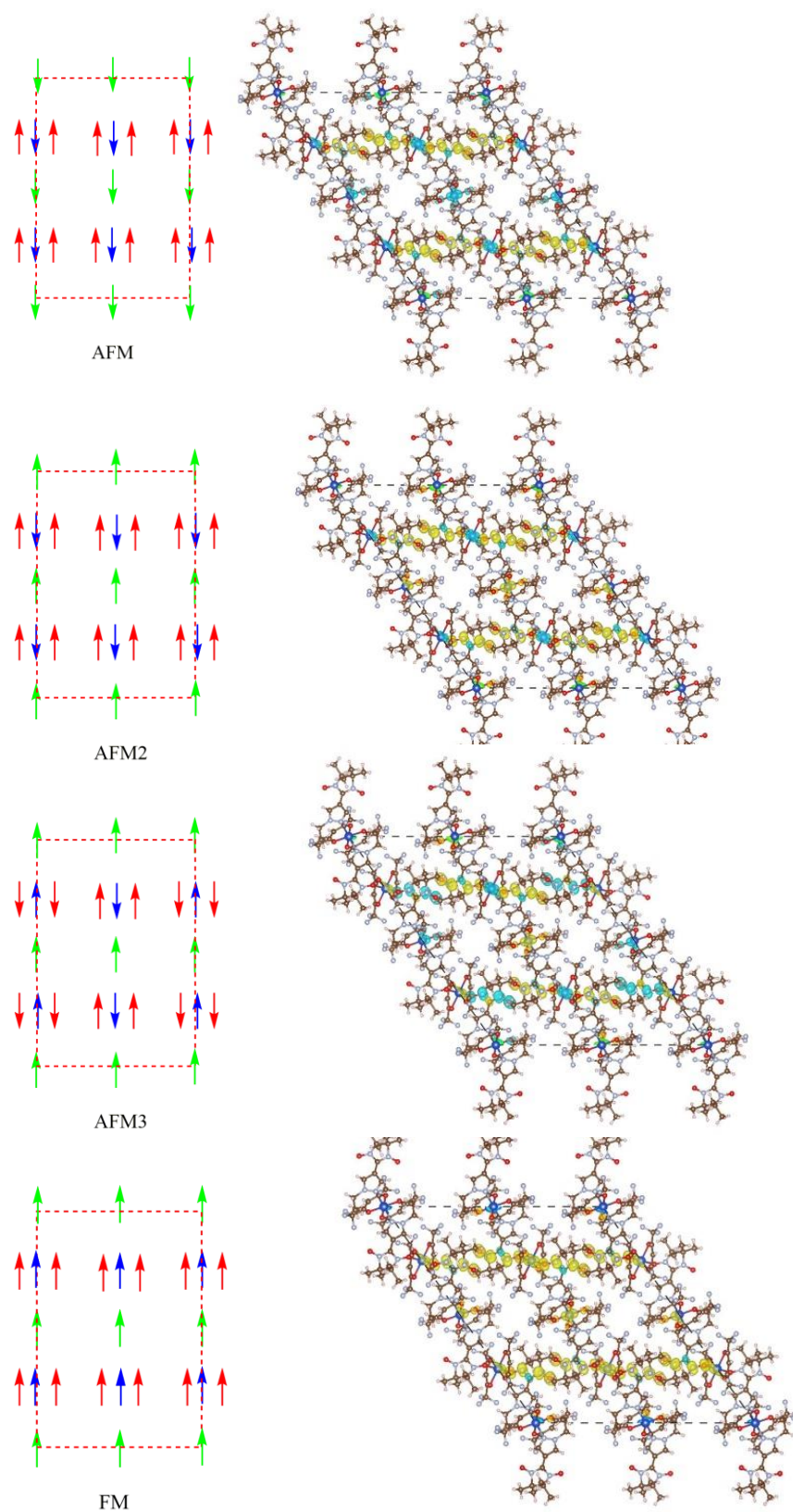


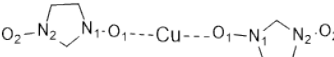
Figure 5. (left) Schematic representation of the considered magnetic solutions for $\text{Cu}(\text{hfac})_2\text{L}^{\text{Pr}}$ (**1**). (right) Spin density maps at low temperature from PBE+ U_d + U_p calculations. View along b axis.

Table 3. Relative energies (per NIT-Cu-NIT...Cu units) of the four magnetic solutions of the $\text{Cu}(\text{hfac})_2\text{L}^{\text{Pr}}$ (**1**) complex using different U values. The magnetic coupling within the spin triad, J , the interaction between the spin triad and the CuO_4N_2 units, J' , and interchain interactions J_{chain} are also reported. All values in cm^{-1} .

Method	Phase	AFM	AFM2	AFM3	FM	J	J'	J_{chain}
PBE+ $U_d(2)$	LT	0.0	1.8	-1.9	2895.2	-1447.6	1.8	-3.8
	HT	0.0	23.3	---	332.6	-166.3	23.3	
PBE+ $U_d(7)$	LT	0.0	0.0	---	1692.9	-846.5	0.0	
	HT	11.1	11.1	---	0.0	5.5	0.0	
PBE+ $U_d(9.8)$	LT	0.0	0.4	---	1097.6	-548.8	0.4	
	HT	21.0	21.0	---	0.0	10.5	0.0	
PBE+ U_d+U_p	LT	0.0	0.0	-1.4	737.0	-368.9	0.0	-2.8
	HT	27.8	27.8	---	0.0	13.5	0.0	

The spin density values on the spin triad atoms are shown in Table 4 for the ground state of each structure at PBE+ U_d+U_p level and represented in Figures 4 and 5. Regarding the nitroxide groups, the spin density is not homogeneously distributed being localized with advantage in the terminal nitroxide groups, in good agreement with the picture provided by our previous calculations at CASSCF/DDCI level^[24] and the spin density maps obtained from polarized neutron diffraction experiments on similar head-to-head nitroxide-Cu-nitroxide systems.^[47] This distribution favors the interactions among neighbour chains mediated just by these terminal NO groups.

Table 4. Spin densities in the ground state at PBE+ U_d+U_p level on N, O and Cu atoms of the spin triad of $\text{Cu}(\text{hfac})_2\text{L}^{\text{R}}$ complexes at low and high temperatures.

						
$\text{Cu}(\text{hfac})_2\text{L}^{\text{R}}\cdot\text{solv}$	phase	Cu	O1	N1	N2	O2
1 R=Pr	LT	-0.811	0.107	0.178	0.168	0.363
	HT	0.876	0.195	0.172	0.171	0.347
2 R=Bu, solv=octane	LT	-0.833	0.109	0.174	0.170	0.369
	HT	0.858	0.212	0.177	0.174	0.328
3 R=Bu, solv=o-xylene	LT	-0.811	0.089	0.170	0.165	0.384
	HT	0.878	0.174	0.169	0.169	0.358

4.2. Evaluation of the magnetic interactions

The evaluation of the interaction parameters from periodic DFT-based calculations relies on the mapping between the magnetic solutions and the diagonal terms of the Heisenberg-Dirac-Van-Vleck (HDVV) Hamiltonian.^{[48],[49]} The HDVV Hamiltonian takes the form

$$\hat{H}_{\text{HDVV}} = -2 \sum_{i < j} J_{ij} \left(\hat{S}_i \hat{S}_j - \frac{1}{4} \hat{I} \right)$$

where \hat{S} is the spin operator, J_{ij} is the coupling constant between the spins in centres i and j and $\hat{1}$ is the identity operator, that multiplied by $1/4$ makes zero the energy of the highest spin multiplicity state. Notice that here the term “centre” is used in a wide sense, since in the case of the nitronyl-nitroxide radicals it refers to a multicentre magnetic site with $S=1/2$. Four different magnetic coupling constants can be distinguished: the nitroxide-Cu J and nitroxide-nitroxide J_{NO} interactions inside the spin triad and the interaction between the spin triad and the CuO_4N_2 group, J' . These three interactions are located along the polymer chain, while the interaction between chains is mediated by the terminal nitroxide groups, J_{chain} .

The energy (per NIT-Cu-NIT...Cu units) for each magnetic solution can be related to the interaction parameters as follows:

$$E_{AFM} - E_{FM} = 2J$$

$$E_{AFM2} - E_{FM} = 2J + J'$$

$$E_{AFM3} - E_{FM} = 2J + J' + (J_{\text{chain}}/2)$$

$$E_{AFM4} - E_{FM} = J + J_{NO} + J_{\text{chain}}$$

The J_{NO} interaction has been neglected, since our previous DDCI calculations^[24] on $\text{Cu}(\text{hfac})_2\text{L}^{\text{Bu}}\cdot 0.5\text{C}_8\text{H}_{18}$ (**2**) demonstrated that this interaction is almost null regardless the temperature. The J values obtained at PBE+ U_d+U_p level for the three systems in the LT and HT phases are collected in Table 2. In all cases, the periodic calculations predict a strong antiferromagnetic interaction between nitronyl-nitroxide and Cu spins at LT, in line with a strongly exchange coupled state SS, while this interaction becomes ferromagnetic at HT, as expected for the weakly coupled state WS. The calculations also indicate that the CuO_4N_2 units remain magnetically isolated regardless of the phase.

Comparing with the results obtained for $\text{Cu}(\text{hfac})_2\text{L}^{\text{Bu}}\cdot 0.5\text{C}_8\text{H}_{18}$ (**2**) complex from DDCI calculations on the spin triad ($J = -145.3 \text{ cm}^{-1}$ and 8.7 cm^{-1} for the LT and HT phases, respectively, using the quartet CASSCF(3/3) molecular orbitals in the configuration interaction expansion),^[24] the J constants at PBE+ U_d+U_p level are those in better agreement with the DDCI ones, although always larger in amplitude for both phases. This overestimation is a well-known feature of the DFT-based evaluations of the magnetic coupling constants, extensively discussed in the past for many magnetic binuclear compounds,^{[50],[51],[52],[53],[54]} and also found for the family of $\text{Cu}(\text{hfac})_2\text{L}^{\text{R}}$ breathing crystals.^{[19],[27]} The interchain interaction is antiferromagnetic in nature and of the same order of magnitude than the J value within the spin triads at high temperature. This implies that in the WS state there is not a dominant magnetic interaction, but J and J_{chain} are competing, resulting in a frame of spin states very close in energy, of vital importance for the interpretation of the spin dynamics and the relaxation of the photoinduced WS state.^{[24],[21],[26]} The amplitude of this interaction is indeed in good agreement with previous independent evaluations on isolated nitronyl-nitroxide fragments based on DDCI^[24] and broken-symmetry DFT calculations.^[26]

4.3. Density of states

The density of states (DOS) for the AFM magnetic solutions of the three compounds at low and high temperatures is shown in Figure 6 for PBE+ U_d+U_p and Figures S3-S6 for $\text{Cu}(\text{hfac})_2\text{L}^{\text{Pr}}$ (**1**) complex with different U values. Although there are no experimental data of the band gap magnitude or electric conductivity for any compound of the $\text{Cu}(\text{hfac})_2\text{L}^{\text{R}}$ family, the EPR data

indicate that they do not exhibit a metallic behaviour, then the presence of band gap is implicitly inferred.

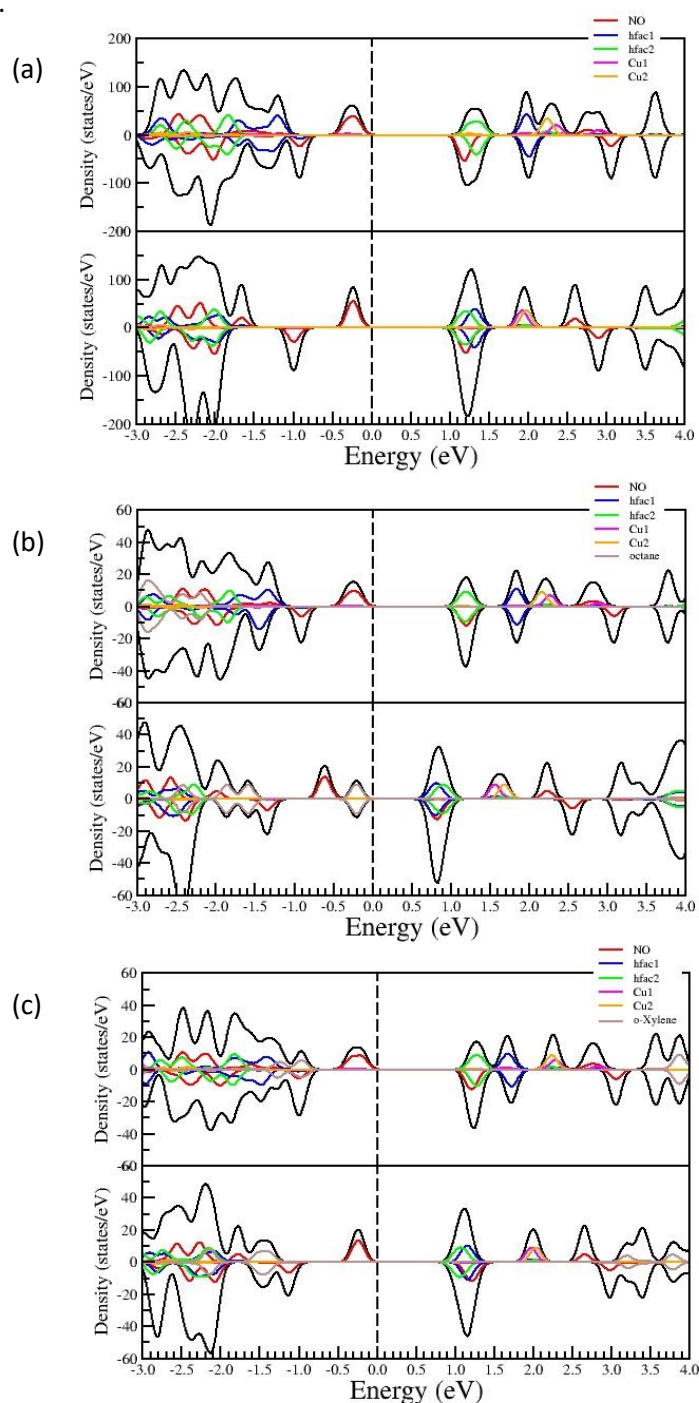


Figure 6. Density of states for the AFM magnetic solution at low (top) and high temperatures (bottom) of (a) $\text{Cu}(\text{hfac})_2\text{L}^{\text{Pr}}$ (**1**) (b) $\text{Cu}(\text{hfac})_2\text{L}^{\text{Bu}}\cdot 0.5\text{C}_8\text{H}_{18}$ (**2**) and (c) $\text{Cu}(\text{hfac})_2\text{L}^{\text{Bu}}\cdot 0.5\text{C}_8\text{H}_{10}$ (**3**) from $\text{PBE}+U_d+U_p$ calculations (black) and projected DOS on the NO groups (red), C and O atoms of the hfac1 (blue) and hfac2 (green) groups, Cu1 (magenta) and Cu2 (orange) atoms and solvent (grey) atoms. The vertical dotted lines represent the Fermi level.

For $U=2$ eV the system presents no band-gap (Figure S3). The three other explored U values for $\text{Cu}(\text{hfac})_2\text{L}^{\text{Pr}}$ at low temperature give a band gap of 0.7 eV for $U=7$ (Figure S4) and $U=9.8$ eV (Figure S5), while the gap slightly increases up to 1 eV in the case of the $\text{PBE}+U_d+U_p$ approach

(Figure S6). When going to the HT structure, the gap is slightly reduced by about 0.2 eV. For all the explored values, the valence band has a major contribution of the nitronyl-nitroxide groups while the low-lying conduction bands are mainly centred on (i) the C and O atoms of the hfac ligands, (ii) on the nitronyl-nitroxide groups, and (iii) on the Cu atoms.

The DOS of the three compounds resulting from the PBE+ U_d+U_p calculations (Figure 6) are very similar in both nature and energy of the low-lying bands. At low temperature, two hfac-based conduction bands can be distinguished: one centered on the isolated CuO_4N_2 units (labeled as hfac2 in Figure 6) at lower energy than the band due to the hfac ligands of the spin triads (labeled as hfac1). These two bands almost collapse at high temperature giving rise to a single band at about 1.2 eV above the Fermi level. This could be related to the fact that the $\text{Cu1-O}_{\text{hfac1}}$ and $\text{Cu2-O}_{\text{hfac2}}$ bond distances become quite similar at HT, while they differ by up to 0.3 Å in the LT phase. The next bands in energy are associated to Cu atoms (Figure 6). These Cu bands suffer a red shift displacement of about 0.2-0.3 eV in the HT phase, being placed at ~2 eV above the Fermi level. This red shift displacement could also be associated to the changes observed on the coordination spheres of the Cu atoms when going from the LT to the HT phases.

The position of the Cu bands depends on the U value (Figures S3-S6). Going from $U(\text{Cu})=7$ eV to $U(\text{Cu})=9.8$ eV moves these Cu bands to higher energy. The same effect is observed in the conduction oxygen-centered band when the PBE+ U_d+U_p approach is employed.

The relative position of the low-lying bands in the DOS provides potentially useful information for the assignment of the UV-vis absorption spectra, in particular a qualitative picture of both the energy and the nature of the electronic transitions in the UV-vis absorption spectra and the bleaching observed in the 500-600 nm region after photoactivation. Figure 3 shows the experimental UV-vis spectrum of $\text{Cu}(\text{hfac})_2\text{L}^{\text{Pr}}$ (**1**) recorded in the 400-900 nm range at different temperatures.^{[13],[22]} The LT and HT phases present quite similar bands in this region, but a distinctive feature of the LT structure is the presence of an intense band at $\lambda=500$ nm, assigned to a (metal-ligand or ligand-metal) charge transfer transition,^{[13],[14]} based on the fact that the Cu-O distances in the spin triads are noticeably modified upon SS \leftrightarrow WS conversion.

Table 5 reports the energy difference at PBE+ U_d+U_p level between the centres of the bands close to the Fermi level for $\text{Cu}(\text{hfac})_2\text{L}^{\text{Pr}}$ complex, mainly the valence band and the low-lying conduction bands. Although qualitative, these energy differences give information about the features observed in the UV-vis spectra and the main changes that could be expected after SS \leftrightarrow WS conversion. Notice that our calculations do not provide information about the transition dipole moments, then the relative intensities (if any) of these bands cannot be anticipated and consequently the corresponding wavelength values in Table 5 are just tentative. The separation between bands of the same nature is reduced (the wavelength required for a transition between them increases) when going from the LT to the HT structure, with the exception of the transition between nitroxide bands, where the trend is the opposite one. The first feature can be related to the bleaching observed in the 500-600 nm region after photoswitching. Particularly remarkable is the energy difference between the nitroxide bands and the Cu centered ones of 2.5 eV (~500 nm) in the LT phase, while the gap between these bands moves to lower energy ~2.2 eV in the HT structure, then larger wavelengths (~570 nm) are required to promote a transition between these two bands when temperature increases.

These two bands could be responsible (assuming a non-negligible oscillator strength) for the $\lambda=500$ nm transition observed at low temperature and distinctive of the strongly coupled SS phase. The periodic calculations suggest that this band could be ascribed to a ligand-to-metal charge transfer transition, from the nitronyl-nitroxide groups to the Cu atoms, both intimately involved in the magnetic properties of the LT and HT structures and the SS \leftrightarrow WS conversion. The charge redistribution between metal and ligands has also been invoked as a key ingredient of the spin transition in spin-crossover Fe(II) compounds.^[55] This is a central result of this work that could help in clarifying the mechanism controlling the photoswitching process.

In the case of the separation between the nitroxide bands and the corresponding nitroxide-nitroxide transitions, the energy difference increases somewhat (the wavelength decreases) when going from LT to HT structures.

The final remark concerns the impact of the +U correction on the energy and nature of the projected DOS. As occurs with the J values, only the DOS at PBE+U_d+U_p level presents significant differences between the LT and HT structures that could be related to the signatures observed in the UV-vis absorption spectra. Then, the U correction of both the Cu 3d and O 2p orbitals is required for a correct description of the Cu(hfac)₂L^R complexes.

Table 5. Energy difference between the centre of the valence band and low-lying conduction bands and wavelengths of the corresponding transition for Cu(hfac)₂L^{Pr} (**1**) complex at PBE+U_d+U_p level.

	Assignment	LT		HT	
		ΔE /eV	λ /nm	ΔE /eV	λ /nm
α -DOS	hfac2 \leftarrow NO	1.54	805	1.41	880
	hfac1 \leftarrow NO	2.23	556	1.55	800
	Cu2 \leftarrow NO	2.48	500	2.14	564
	Cu1 \leftarrow NO	2.59	479	2.20	580
	NO \leftarrow NO	2.99	415	3.12	397
β -DOS	NO \leftarrow NO	2.09	593	2.19	566
	hfac2 \leftarrow NO	2.23	556	2.19	566
	hfac1 \leftarrow NO	2.90	428	2.30	539

5. Conclusions

The Cu(hfac)₂L^R breathing crystals family manifests thermal magnetostructural transitions and LIESST-like phenomena quite similar to those experienced by the classical spin-crossover compounds. While a large amount of research has been devoted to the characterization and understanding of the thermally induced spin transition, much less is known about the optical properties of these copper-nitroxide based molecular magnets.

This work provides information about the electronic structure of the whole crystal of three members of the $\text{Cu}(\text{hfac})_2\text{L}^{\text{R}}$ family, relevant for the assignment of the UV-vis spectra and the rationalization of the photoinduced switching. The results of a set of periodic DFT+U based calculations in the two limit phases concern the relative stability of the different spin arrangements in the crystal and the amplitude and nature of the magnetic interaction in these heterospin complexes. They are consistent with the EPR data and the observed changes of the magnetic moment with temperature. Additionally, the density of states gives insights on the states potentially accessible by electronic transitions in the UV-vis range that could be involved in the photoswitching process. The similarities found in the DOS for the three considered compounds suggest the possibility of light-induced spin switching for other members of the breathing crystal family for which this phenomenon has still not been reported. Work is in progress to accurately quantify the transition energies and in particular the oscillator strengths for transitions in the UV-vis range by means of CASSCF/CASPT2 calculations on the spin triad.

The study highlights the potential of the PBE+U calculations on the understanding of the optical properties of these systems, and its conclusions could be relevant not only for the particular compounds analysed, but for many other $\text{Cu}(\text{hfac})_2\text{L}^{\text{R}}$ complexes.

Acknowledgments

The authors acknowledge the financial support provided by the Ministerio de Economía y Competitividad (Spain) and FEDER funds through the projects CTQ2015-69019-P (MINECO/FEDER) and access to the resources of the Red Española de Supercomputación (RES) through project nº QCM-2017-3-0033. R. Sánchez-de-Armas thanks VPPI-US for the financial support.

Supporting Information

Structural parameters and unit cell representation for compounds 1-3. Relative energies of the four magnetic solutions and interaction parameters for $\text{Cu}(\text{hfac})_2\text{L}^{\text{Bu}}\cdot 0.5\text{C}_8\text{H}_{18}$ and $\text{Cu}(\text{hfac})_2\text{L}^{\text{Bu}}\cdot 0.5\text{C}_8\text{H}_{10}$ complexes (**2** and **3**) using different U values. Spin density maps of compound **3**. Density of states (DOS) for $\text{Cu}(\text{hfc})_2\text{L}^{\text{Pr}}$ obtained from PBE+U_d calculations for LT and HT phases. VASP input file for the FM solution of compound 1.

References

- [1] O. Sato, *Nature Chemistry* **2016**, *8*, 644.
- [2] *Spin-crossover materials. Properties and applications*, Wiley, **2013**, p.
- [3] A. Bousseksou, G. Molnár, L. Salmon and W. Nicolazzi, *Chemical Society Reviews* **2011**, *40*, 3313-3335.
- [4] S. Decurtins, P. Gülich, C. P. Köhler, H. Spiering and A. Hauser, *Chemical Physics Letters* **1984**, *105*, 1-4.

- [5] P. Gütlich and A. Hauser, *Coordination Chemistry Reviews* **1990**, *97*, 1-22.
- [6] S. Hayami, Z.-z. Gu, M. Shiro, Y. Einaga, A. Fujishima and O. Sato, *Journal of the American Chemical Society* **2000**, *122*, 7126-7127.
- [7] F. Lanfranc de Panthou, E. Belorizky, R. Calemczuk, D. Luneau, C. Marcenat, E. Ressouche, P. Turek and P. Rey, *Journal of the American Chemical Society* **1995**, *117*, 11247-11253.
- [8] A. Caneschi, P. Chiesi, L. David, F. Ferraro, D. Gatteschi and R. Sessoli, *Inorganic Chemistry* **1993**, *32*, 1445-1453.
- [9] V. I. Ovcharenko and E. G. Bagryanskaya in *Breathing Crystals from Copper Nitroxyl Complexes*, **2013**, pp. 239-280.
- [10] M. V. Fedin, S. L. Veber, E. G. Bagryanskaya and V. I. Ovcharenko, *Coordination Chemistry Reviews* **2015**, *289-290*, 341-356.
- [11] M. Fedin, S. Veber, I. Gromov, K. Maryunina, S. Fokin, G. Romanenko, R. Sagdeev, V. Ovcharenko and E. Bagryanskaya, *Inorganic Chemistry* **2007**, *46*, 11405-11415.
- [12] F. Matvey, O. Victor, S. Renad, R. Edward, L. Wolfgang and B. Elena, *Angewandte Chemie International Edition* **2008**, *47*, 6897-6899.
- [13] W. Kaszub, A. Marino, M. Lorenc, E. Collet, E. G. Bagryanskaya, E. V. Tretyakov, V. I. Ovcharenko and M. V. Fedin, *Angewandte Chemie-International Edition* **2014**, *53*, 10636-10640.
- [14] I. Y. Barskaya, S. L. Veber, E. A. Suturina, P. S. Sherin, K. Y. Maryunina, N. A. Artiukhova, E. V. Tretyakov, R. Z. Sagdeev, V. I. Ovcharenko, N. P. Gritsan and M. V. Fedin, *Dalton Transactions* **2017**, *46*, 13108-13117.
- [15] S. L. Veber, M. V. Fedin, K. Y. Maryunina, A. Potapov, D. Goldfarb, E. Reijerse, W. Lubitz, R. Z. Sagdeev, V. I. Ovcharenko and E. G. Bagryanskaya, *Inorganic Chemistry* **2011**, *50*, 10204-10212.
- [16] S. L. Veber, M. V. Fedin, A. I. Potapov, K. Y. Maryunina, G. V. Romanenko, R. Z. Sagdeev, V. I. Ovcharenko, D. Goldfarb and E. G. Bagryanskaya, *Journal of the American Chemical Society* **2008**, *130*, 2444-2445.
- [17] E. V. Tretyakov, S. E. Tolstikov, A. O. Suvorova, A. V. Polushkin, G. V. Romanenko, A. S. Bogomyakov, S. L. Veber, M. V. Fedin, D. V. Stass, E. Reijerse, W. Lubitz, E. M. Zueva and V. I. Ovcharenko, *Inorganic Chemistry* **2012**, *51*, 9385-9394.
- [18] G. V. Romanenko, K. Y. Maryunina, A. S. Bogomyakov, R. Z. Sagdeev and V. I. Ovcharenko, *Inorganic Chemistry* **2011**, *50*, 6597-6609.
- [19] V. I. Ovcharenko, G. V. Romanenko, K. Y. Maryunina, A. S. Bogomyakov and E. V. Gorelik, *Inorganic Chemistry* **2008**, *47*, 9537-9552.
- [20] M. V. Fedin, S. L. Veber, G. V. Romanenko, V. I. Ovcharenko, R. Z. Sagdeev, G. Klihm, E. Reijerse, W. Lubitz and E. G. Bagryanskaya, *Physical Chemistry Chemical Physics* **2009**, *11*, 6654-6663.
- [21] M. V. Fedin, K. Y. Maryunina, R. Z. Sagdeev, V. I. Ovcharenko and E. G. Bagryanskaya, *Inorganic Chemistry* **2012**, *51*, 709-717.
- [22] M. V. Fedin, E. G. Bagryanskaya, H. Matsuoka, S. Yamauchi, S. L. Veber, K. Y. Maryunina, E. V. Tretyakov, V. I. Ovcharenko and R. Z. Sagdeev, *Journal of the American Chemical Society* **2012**, *134*, 16319-16326.
- [23] I. Y. Drozdoyuk, S. E. Tolstikov, E. V. Tretyakov, S. L. Veber, V. I. Ovcharenko, R. Z. Sagdeev, E. G. Bagryanskaya and M. V. Fedin, *The Journal of Physical Chemistry A* **2013**, *117*, 6483-6488.
- [24] J. Jung, B. L. Guennic, M. V. Fedin, V. I. Ovcharenko and C. J. Calzado, *Inorganic Chemistry* **2015**, *54*, 6891-6899.
- [25] S. Vancoillie, L. Rulíšek, F. Neese and K. Pierloot, *The Journal of Physical Chemistry A* **2009**, *113*, 6149-6157.
- [26] M. V. Fedin, S. L. Veber, K. Y. Maryunina, G. V. Romanenko, E. A. Suturina, N. P. Gritsan, R. Z. Sagdeev, V. I. Ovcharenko and E. G. Bagryanskaya, *Journal of the American Chemical Society* **2010**, *132*, 13886-13891.
- [27] V. A. Morozov, M. V. Petrova and N. N. Lukzen, *AIP Advances* **2015**, *5*, 087161.

- [28] V. I. Ovcharenko, S. V. Fokin, G. V. Romanenko, Y. G. Shvedenkov, V. N. Ikorskii, E. V. Tretyakov and S. F. Vasilevskii, *Journal of Structural Chemistry* **2002**, *43*, 153-167.
- [29] V. I. Ovcharenko, K. Y. Maryunina, S. V. Fokin, E. V. Tretyakov, G. V. Romanenko and V. N. Ikorskii, *Russian Chemical Bulletin* **2004**, *53*, 2406-2427.
- [30] M. V. Fedin, S. L. Veber, I. A. Gromov, V. I. Ovcharenko, R. Z. Sagdeev, A. Schweiger and E. G. Bagryanskaya, *Journal of Physical Chemistry A* **2006**, *110*, 2315-2317.
- [31] M. V. Fedin, S. L. Veber, I. A. Gromov, V. I. Ovcharenko, R. Z. Sagdeev and E. G. Bagryanskaya, *Journal of Physical Chemistry A* **2007**, *111*, 4449-4455.
- [32] G. Kresse and J. Hafner, *Physical Review B* **1993**, *47*, 558-561.
- [33] G. Kresse and J. Hafner, *Physical Review B* **1994**, *49*, 14251-14269.
- [34] G. Kresse, Furthmuller, J., *Computational Materials Science* **1996**, *6*, 15-50.
- [35] G. Kresse and J. Furthmuller, *Physical Review B* **1996**, *54*, 11169-11186.
- [36] a) J. P. Perdew, K. Burke and M. Ernzerhof, *Physical Review Letters* **1996**, *77*, 3865-3868; b) J. P. Perdew, K. Burke and M. Ernzerhof, *Physical Review Letters* **1997**, *78*, 1396-1396.
- [37] P. E. Blochl, *Physical Review B* **1994**, *50*, 17953-17979.
- [38] G. Kresse, Joubert, D., *Physical Review B* **1999**, *59*, 1758-1775.
- [39] S. L. Dudarev, G. A. Botton, S. Y. Savrasov, C. J. Humphreys and A. P. Sutton, *Physical Review B* **1998**, *57*, 1505-1509.
- [40] S. V. Streltsov, M. V. Petrova, V. A. Morozov, G. V. Romanenko, V. I. Anisimov and N. N. Lukzen, *Physical Review B* **2013**, *87*, 024425.
- [41] P. Verma, R. Maurice and D. G. Truhlar, *The Journal of Physical Chemistry C* **2016**, *120*, 9933-9948.
- [42] C. Franchini, R. Podloucky, J. Paier, M. Marsman and G. Kresse, *Physical Review B* **2007**, *75*, 195128.
- [43] A. Sorokin, M. A. Iron and D. G. Truhlar, *Journal of Chemical Theory and Computation* **2008**, *4*, 307-315.
- [44] C. J. Calzado, N. C. Hernandez and J. F. Sanz, *Physical Review B* **2008**, *77*, 045118.
- [45] H. J. Monkhorst and J. D. Pack, *Physical Review B* **1976**, *13*, 5188-5192.
- [46] A. Tkatchenko and M. Scheffler, *Physical Review Letters* **2009**, *102*, 073005.
- [47] E. Ressouche, J. X. Boucherle, B. Gillon, P. Rey and J. Schweizer, *Journal of the American Chemical Society* **1993**, *115*, 3610-3617.
- [48] I. D. R. Moreira, C. J. Calzado, J. P. Malrieu and F. Illas, *Physical Review Letters* **2006**, *97*, 087003.
- [49] I. D. R. Moreira, C. J. Calzado, J. P. Malrieu and F. Illas, *New Journal of Physics* **2007**, *9*, 369.
- [50] J. P. Malrieu, R. Caballol, C. J. Calzado, C. de Graaf and N. Guihery, *Chemical Reviews* **2014**, *114*, 429-492.
- [51] R. Eliseo, *Journal of Computational Chemistry* **2011**, *32*, 1998-2004.
- [52] R. Valero, R. Costa, I. de P.R. Moreira, D. G. Truhlar and F. Illas, *The Journal of Chemical Physics* **2008**, *128*, 114103.
- [53] C. J. Cramer and D. G. Truhlar, *Physical Chemistry Chemical Physics* **2009**, *11*, 10757-10816.
- [54] P. Rivero, I. De P.R. Moreira, F. Illas and G. E. Scuseria, *The Journal of Chemical Physics* **2008**, *129*, 184110.
- [55] M. Kepenekian, B. Le Guennic and V. Robert, *Journal of the American Chemical Society* **2009**, *131*, 11498-11502.